Macromolecules **2001,** *34,* 7809−7816

Organization and Orientation of a Triblock Copolymer Poly(ethylene glycol)-*b*-poly(*p*-phenylene ethynylene)-*b*-poly(ethylene glycol) and Its Blends in Thin Films

W. Y. Huang, S. Matsuoka, T. K. Kwei,* and Y. Okamoto*

Polymer Research Institute, Polytechnic University, 6 Metrotech Center, Brooklyn, New York 11201

Xuesong Hu, Miriam H. Rafailovich, and Jonathan Sokolov

Department of Materials Science and Engineering, State University of New York,
Stony Brook, New York 11794

Received March 1, 2001; Revised Manuscript Received July 26, 2001

ABSTRACT: Molecular organization and orientation in thin films (∼100 nm) of a triblock copolymer, PPEPEG, composed of a rigid, π-conjugated middle block poly(phenyleneethynylene), PPE, and two poly(ethylene glycol) end blocks, PEG, were studied by fluorescence, secondary ion mass spectroscopy (SIMS), and atomic force microscopy (AFM). Fluorescence polarization studies of the triblock copolymer and its blends with poly(methyl methacrylate) (PMMA) led to the conclusion that the triblock copolymer molecules were oriented perpendicularly to the silicon substrate surface. Orientation of molecules in the vertical direction was confirmed by measurement of the oxygen depth profile of the film with the use of SIMS. Copolymer molecules in large fraction of PMMA (∼2 wt % in PMMA) were molecularly dispersed to give rise to high fluorescence emission intensity at a wavelength characteristic of nonaggregated chains. The reinforced action of this rigid polymer for PMMA was obtained. The secant modulus of the 2 wt % blend in a tensile test was 5.7 times the value of PMMA.

Introduction

This investigation is the outgrowth of an ongoing study of the fluorescence of π-conjugated rigid polymers. We reported earlier that when poly(2-benzoyl-1,4-phenylene), PBP, was blended with poly(methyl methacrylate), PMMA, the photoluminescence intensities of thin films increased significantly.[1] The highest intensity increase, ∼80-fold, was observed when the weight ratio of PBP/PMMA was 1/99. Larger percentages of PBP in the blend films caused a reduction in intensity from the highest value. It was reasoned that dilution of the conjugated rodlike chains by a nonphotoactive ingredient reduced intermolecular contact and minimized the aggregation effect,[1,2] which was responsible for low emission intensity.

In the pursuit of strongly emissive materials, we and other researchers have synthesized poly(phenyleneethynylene)s,[3−15] PPE. The highly conjugated structure indeed showed strong emission in dilute solutions, but fluorescence in the solid state was again marred by the aggregation effect.[3,7,8] In hopes of duplicating the beneficial dilution effect on fluorescence seen in the PBP/PMMA system, we have prepared 2,5 octyl(*p*-phenyleneethynylene) and blended with PMMA. However, the two polymers were completely immiscible, and there was no enhancement in fluorescence intensity. We then synthesized a ABA type triblock copolymer with the PPE chromophores as the middle block and poly(ethylene glycol), PEG, as the two end blocks (Figure 1) because it was well-known in the literature[16−18] that PEG was miscible with PMMA, and our past work had shown that another ABA triblock copolymer with PEG as end blocks interacted favorably with PMMA.[19] Our initial interest in fluorescence enhancement soon led to the investigation of the orientation of the triblock copolymer in thin films of its blends, using fluorescence polarization, secondary ion mass spectroscopy, and atomic force microscopy. There are several reports in the literature[20−27] on the orientation of block copolymers in thin films. Our results with the PEG-*b*-PPE-*b*-PEG copolymer and its blends appear to be novel and are reported here.

Experimental Section

Materials. All chemicals used in this study were purchased from Aldrich Chemicals Co. Spectroscopic grade toluene was used for preparing binary blends. *o*-Dichlorobenzene was purchased as dry solvent and used as received. Tetrahydrofuran (THF) was dried over sodium benzophenone and distilled under an argon atmosphere before use. Triethylamine (TEA) was dried over KOH, and toluene was dried over CaH_2. Both solvents were then distilled under argon atmosphere and deoxygenated by purging with argon for 30 min before use in synthesis.

Poly(ethylene glycol)$_{10}$ methacrylate was purchased from Aldrich Chemicals Co. Poly(methyl methacrylate) (PMMA)($M_w = 10\,000$) and deuterated polystyrene(PSD) ($M_w = 10\,000$) were purchased from Polyscience Co. The triblock copolymer poly(ethylene glycol)-*block*-poly(2,5-dioctyl *p*-phenyleneethynylene)-*block*-poly(ethylene glycol) (PPEPEG) was synthesized, and the structure is shown in Figure 1. The number-average degree of polymerization (P_n) in PPEPEG reported here was determined as 40.[3]

Characterization. Differential scanning calorimetry (DSC) was run on a DSC 2920 module in conjunction with the TA Instrument 5100 system. All melting temperature (T_m) and glass transition (T_g) were obtained using DSC, where the peak maximum and inflection point of the glass transition were taken as T_m and T_g, respectively. The fluorescence spectra were collected by using Perkin-Elmer LS-50B luminescence spectrophotometer with and without polarizers, where the solid-state emission was performed in the 30°/60° angle geometry with spin-coated films about 100 nm in thickness. An atomic force microscope (AFM, Digital Nanoscope III) was employed

10.1021/ma010375k CCC: $20.00

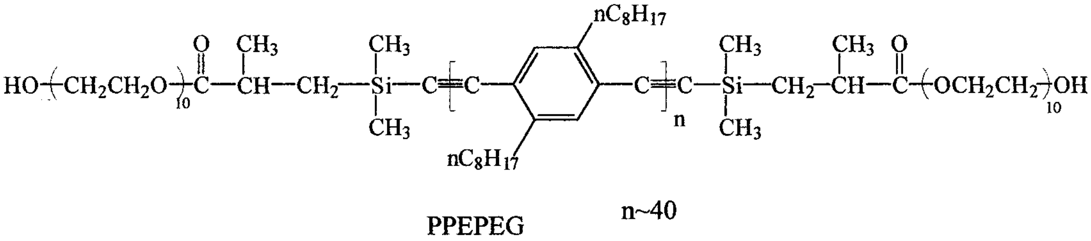

Figure 1. Structure of triblock (PPEPEG).

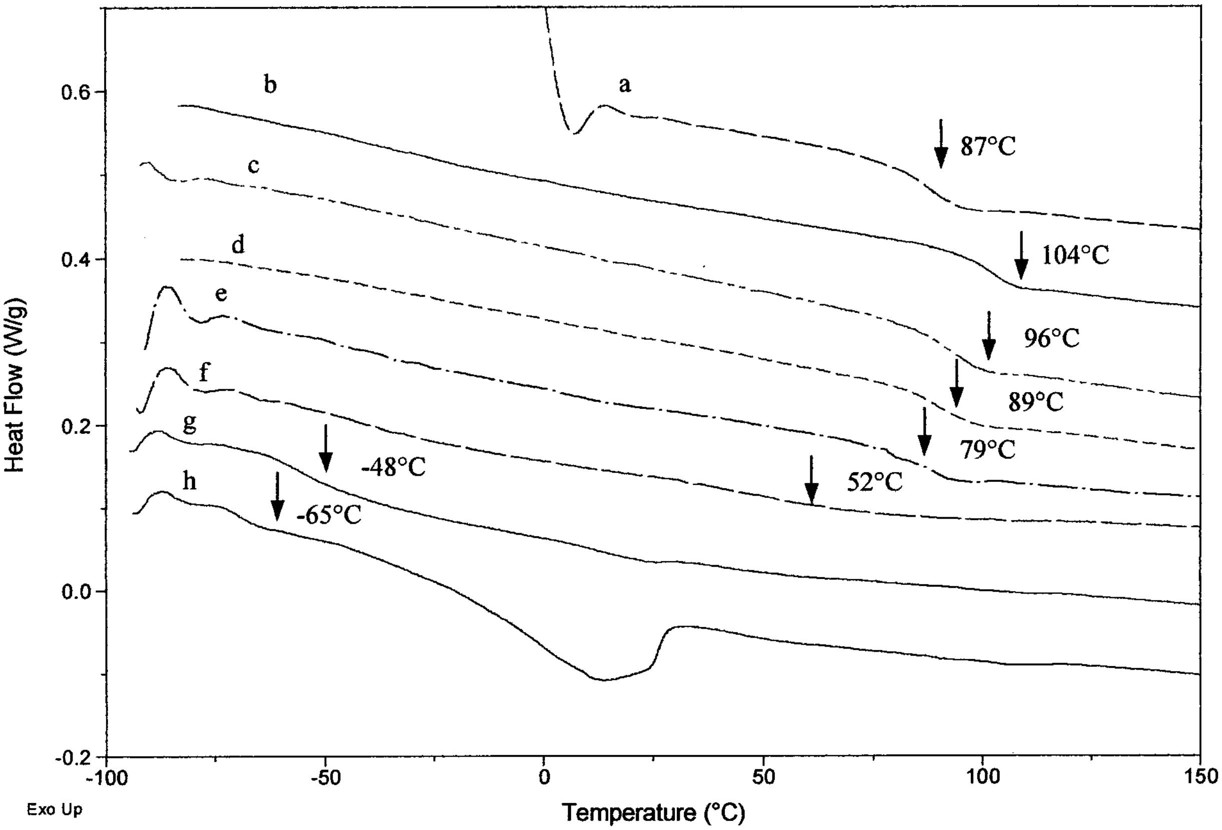

Figure 2. DSC thermograms for (a) pristine PMMA and (b) 2/98, (c) 5/95, (d) 10/90, (e) 20/80, (f) 50/50, (g) 80/20 PPEPEG/PMMA binary blends, and (h) pristine PPEPEG.

to observe morphological and frictional features of the polymer thin films. Secondary ion mass spectroscopy (SIMS) measurements of depth profile of thin films were carried out on an Atomika 6000 SIMS instrument equipped with a negative argon ion beam rastering the sample surface at an operating voltage of 2 kV and a base pressure of 1.3×10^{-6} Pa. In the dynamic SIMS mode, selected secondary ions are monitored as a function of sputtering time, yielding a concentration vs depth profile. The use of SIMS in depth profiling polymer films is reviewed in ref 28, and the interested reader is referred to this paper for more details. It should be noted that the oxygen depth profile is sensitive to the presence or absence of a native oxide layer on the substrate. We therefore utilized silicon substrates precleaned with HF, wherein the native oxide layer was stripped and the surface exposed to the polymer was a passivated SiH. Optical quality thin films of polymers were obtained by spin-coating from toluene solutions onto silicon substrates. The films used in SIMS measurement were covered with a thin layer (~30 nm) of deuterated polystyrene on the top in order to eliminate the unstable data collection at the early stage of the measurement. All the films were dried at 50 °C for 24 h in a vacuum, and their thicknesses were determined by a Rudolph Research Inc. Auto El null point ellipsometry before measurement. Several different film thicknesses ranging from 50 to 350 nm were prepared and studied. However, we focus our attention only on thickness in the range 100−200 nm.

Results and Discussion

I. Molecular Origanization in Thick Films (~100 μm). Before we studied molecular organization and orientation of triblock copolymer molecules in thin films, we have first investigated their organization in thick films in hopes that the information so obtained may serve as a useful guide to the understanding of the thin film structure. Previously, we studied blends[29,30]of a diblock copolymer with a series of homopolymers and were able to obtain information about the phase behaviors in these blends by analyzing the multiple glass transition temperatures. A similar approach was adopted in the present study although, as we shall see, only one T_g could be determined for each blend.

The glass transition temperature, T_g, of the PEG microphase was determined by DSC to be −65 °C; melting of the end block was indicated by a broad endotherm at 13−25 °C (Figure 2). The T_g of the rigid PPE middle block was too high to be detected in our experiment, which was stopped at 250 °C.

Table 1. Transition Temperatures of PPEPPEG/PMMA Binary Blends

binary blends (wt %) PPEPEG/PMMA	100/0	80/20	50/50	20/80	10/90	5/95	2/98	0/100
glass transition temp (°C)	−65	−48	52	79	89	96	104	87
melting temp (°C)	13−25	24	n	n	n	n	n	n

The T_g of PMMA ($M_w \sim 10\ 000$) was seen clearly at 87 °C in the DSC scan. In the 80/20 triblock/PMMA blend, the T_g of the PEG segments increased to −48 °C, obviously due to the mixing of PEG and PMMA segments. According to current theories, in homopolymers−block copolymer blends in which the homopolymers interact favorably with one of the blocks, the homopolymer, in this case PMMA, if present in minor amounts, will “dissolve” in the miscible microphase, in this case PEG. The mechanism of phase separation is called microphase separation and seems to be applicable to the 80/20 blend. As a result of the disruption of packing in the PEG microphase, the melting endotherm became very shallow, although the melting temperature did not change materially.

As the concentration of the copolymer decreased further, the T_g of the PEG−PMMA phase continued to increase (Table 1). At around 50% PMMA and certainly at 80% the homopolymer becomes the continuous phase and the PPE microphases are dispersed in the matrix via the solubilizing action of PEG. The progressive increase of T_g of the blend with PMMA concentration can be readily interpreted as the result of decreasing amount of PEG embedded in the PMMA matrix. Interestingly, in the 10/90, 5/95, and 2/98 blends, the T_g values exceeded that of PMMA. This reinforcement action can occur only if some of the triblock copolymer chains are detached from the PPE microphase and become molecularly dispersed in PMMA so that the rigid PPE block contributes to the elevation of T_g. The PPE microphases, however, do not completely disintegrate, as shall be seen in the section on fluorescence. It is noteworthy that the 2 wt % blend shows the highest T_g at 104 °C, with the inference that molecular dispersion of the triblock copolymer is most efficient in this blend. The reinforcement action also manifests itself in mechanical properties; the secant modulus of the 2 wt % blend in a tensile test is 5.7 times the value for PMMA.

II. Organization and Orientation in Thin Films (~100 nm). A. Fluorescence Properties. The fluorescence emission spectra of the triblock copolymer and its blends are shown in Figure 3. In Figure 3A, a different intensity scale was used for each curve with the sole purpose of showing the peak positions clearly. The spectrum of the triblock copolymer shows a broad peak with λ_{max} at 500 nm. For the 50 wt % blend, the emission maximum is also at 500 nm and a small shoulder appears at ~460 nm. The 10 wt % blend shows an additional emission near 400 nm, which becomes prominent in the 2 wt % blend. When the emission intensities are normalized in Figure 3B, the high emission intensity of the 2 wt % blend stands in sharp contrast with that of the pristine triblock copolymer.

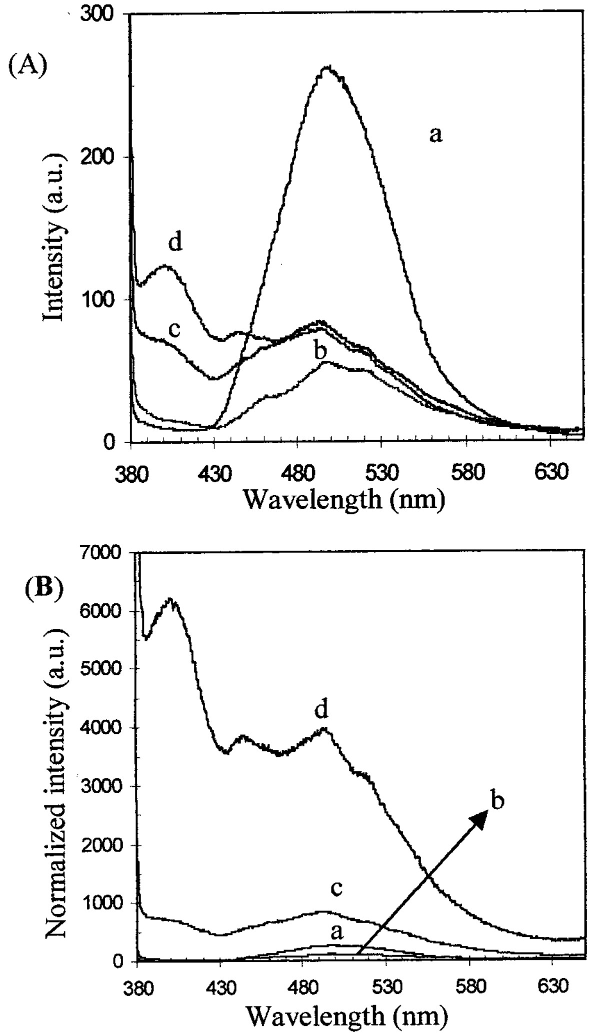

Figure 3. (A) Fluorescence emission spectra of PPEPEG and PMMA blend films: (a) pristine PPEPEG, (b) 50% PPEPEG, (c) 10% PPEPEG, and (d) 2% PPEPEG. (B) Intensities in (A) were normalized with PPEPEG.

The λ_{max} at 500 nm, when compared with 420 nm in dilute solutions, in which the chromophores are far apart, can be designated as the response of aggregates. The low emission intensity of the triblock copolymer film is then the outcome of aggregation quenching. In the 2 wt % blend, emission at 500 nm remains. This indicates that aggregates are present in this “dilute” blend; the higher intensity is due to reduced concentration quenching among aggregates since they are fewer in number and are distant from each other. The 400 nm emission in the 2 wt % blend, which is close to the peak position in dilution solutions, can be readily assigned to triblock chains in the “isolated” state with attendant strong emission intensity. (λ_{max} in dilute solutions is at 420 nm; the slightly longer wavelength is due to the solvation effect which generally causes Stokes shift of 20−30 nm.) The shoulder at 460 nm in curve d probably represents the intermediate state of aggregation. It is also worthy of mention that the presence of isolated chains in the 2 wt % blend is in complete accord with the conclusion reached from T_g measurements of thick films. With the above interpretation in mind, we conclude that the chromophores in the 50 wt % blend are also highly aggregated (curve b), but in the 10 wt % blend the aggregates are further apart and a small number of “isolated” chains may be present because there is indication of a weak emission at 400 nm. The combination of T_g and fluorescence results provides rich information about phase relationship in the blends.

Scheme 1. Schematic Presentation of Relationship between Molecular Orientations and Polarized Light Intensities

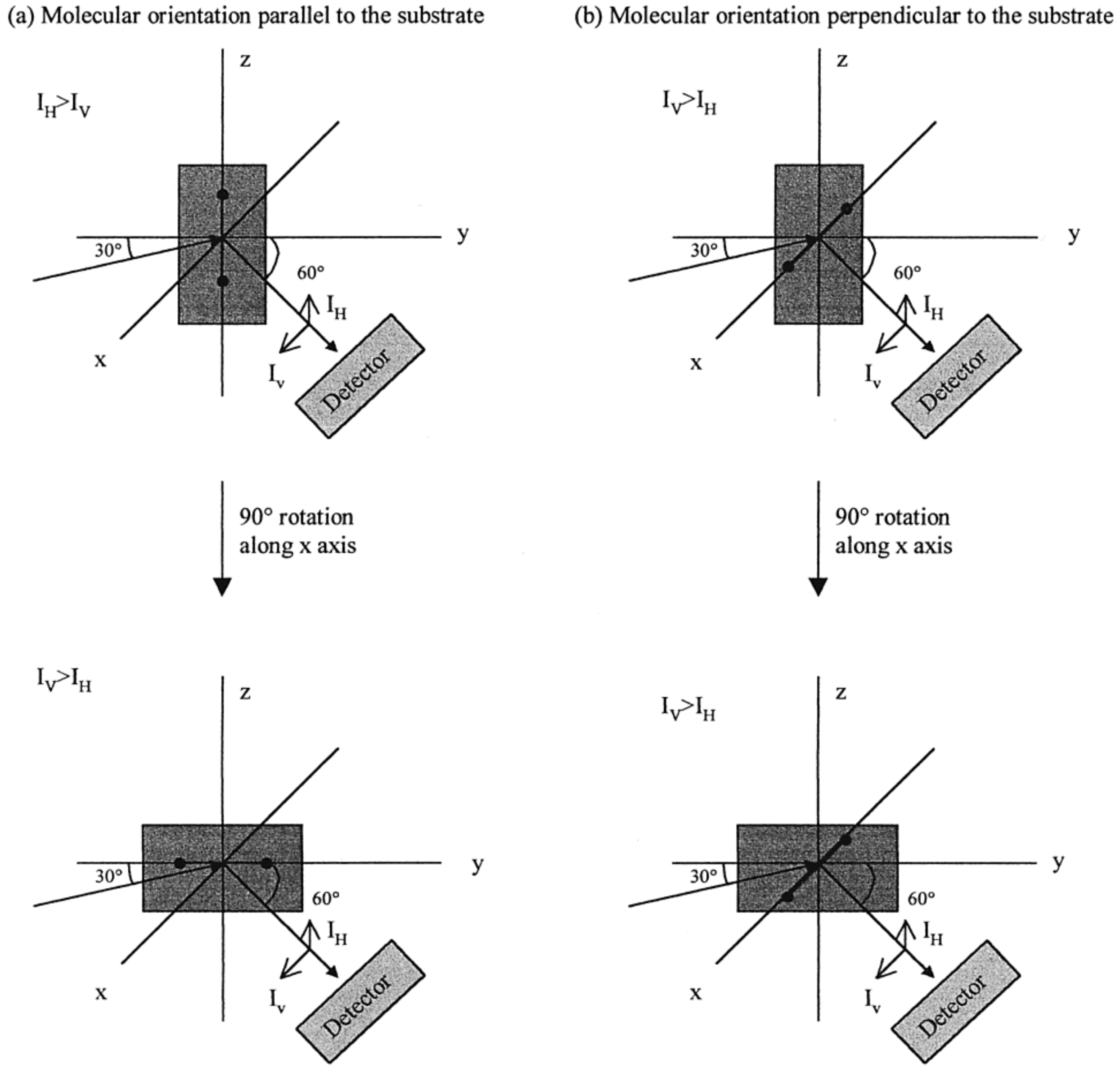

B. Fluorescence Polarization Measurement. We then repeated the experiments with the same excitation (nonpolarized) wavelength of 360 nm but recorded the emission spectra with vertically and horizontally polarized detectors. For illustration, a schematic presentation of the relationship between molecular orientations and polarized light intensities is shown in Scheme 1. In Scheme 1, let I_0 be the emission in the direction of molecular long axis and I_1 be the short axis. I in the case of top (a), $I_V = I_1 \sin 60° + I_1 \cos 60° = (1.732/2)I_1 + (1/2)I_1 \approx 1.37I_1$ and $I_H = I_0$. For a polymer, it is reasonable to assume $I_0 > 1.37I_1$; therefore, $I_H > I_V$. While, in the case of the bottom (a), $I_H = I_1$ and $I_V = I_0 \sin 60° + I_1 \cos 60° = (1.732/2)I_0 + (1/2)I_1 > I_1$, i.e., $I_V > I_H$. On the other hand, if the molecular orientation is perpendicular to the substrate (Scheme 1b), in the both top and bottom cases, $I_H = I_1$ and $I_V = I_0 \sin 30° + I_1 \cos 30° = (1/2)I_0 + (1.732/2)I_1 > I_1$; therefore, $I_V > I_H$. We performed the rotation experiment and confirmed the vertical orientation. We then repeated the experiment with the same excitation (nonpolarized) wavelength of 360 nm but recorded the emission spectra with vertically and horizontally polarized detectors. The results are shown in Figure 4. In Figure 4a, the intensities I_V and I_H for the PPE itself are identical; i.e., there is no preferred orientation of the molecule. However, for the triblock copolymer and its 50 and 2 wt % blends, I_V exceeds I_H. These observations differ from literature reports on diblock copolymers for which I_H values are greater than I_V values, leading to the conclusion that the molecules lie parallel to the surface. Our results, on the other hand, suggest that the molecules are preferably oriented perpendicularly to the surface.

C. Secondary Ion Mass Spectroscopy (SIMS). We also investigated the orientation of the triblock copolymer film on silicon surface using SIMS. The method provides information on the depth profile of oxygen atoms from which the orientation of the chain can be readily ascertained. If the chains are horizontally oriented, the oxygen profile is expected to be uniform throughout the depth of the film. On the other hand, vertically oriented chains would produce a completely different oxygen profile because the middle block con-

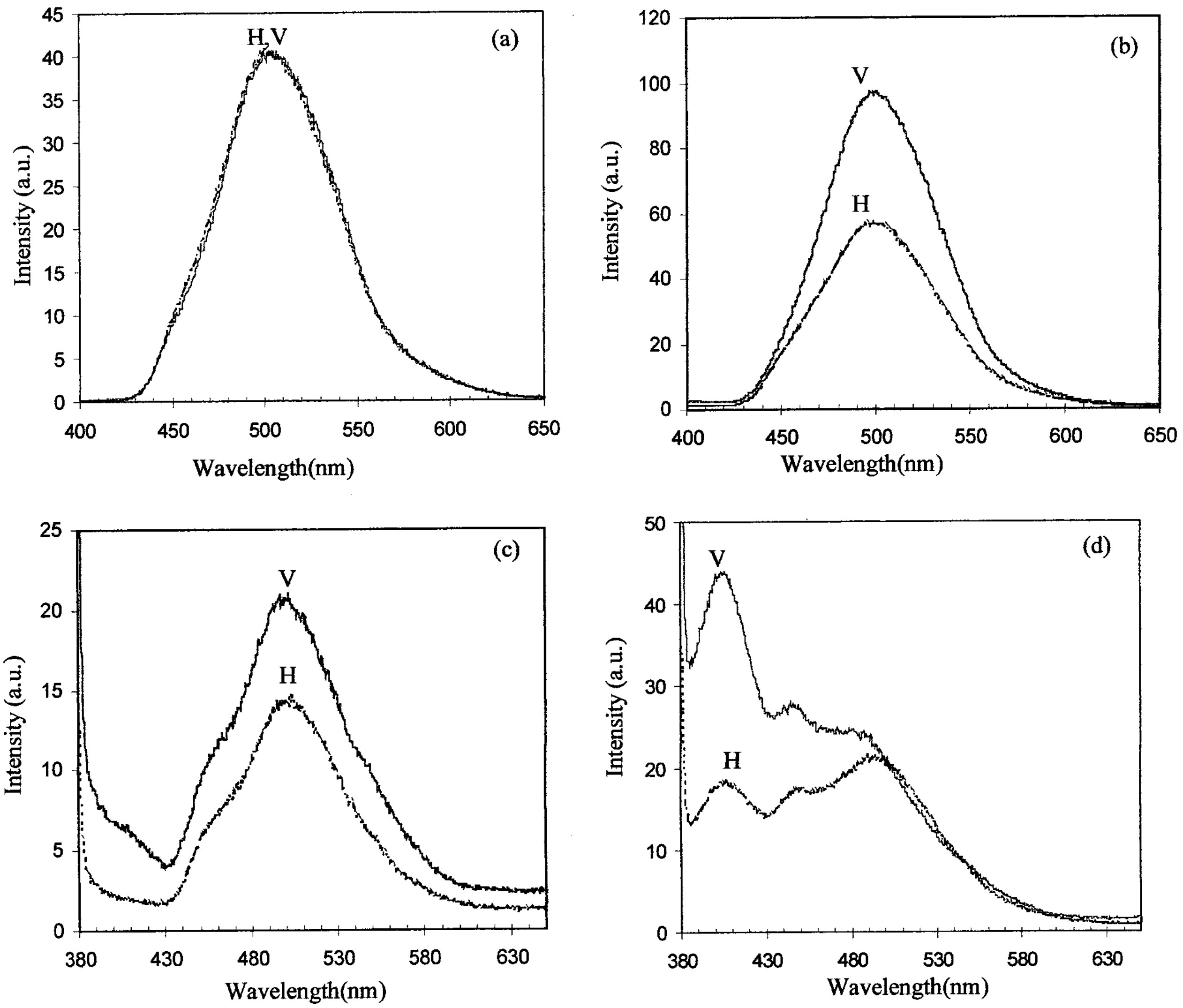

Figure 4. Emission spectra recorded with vertical polarized (V) and horizontal polarized (H) detection under isotropic excitation at 360 nm of (a) PPE pristine film, (b) PPEPEG pristine film, (c) 50/50 PPEPEG/PMMA blend film, and (d) 2/98 PPEPEG/PMMA blend film.

tained no oxygen. The experimental results are shown in Figure 5a for the triblock copolymer. The oxygen count increases immediately after the depletion of the deuterated polystyrene layer. The thickness of the oxygen-rich region near the top of the film surface is ~15 nm. The next oxygen-rich region appears near the bottom surface with a thickness of about 20 nm. The top and bottom regions with high oxygen densities are separated by a middle region, about 35 nm in thickness, of lower oxygen content. Such a depth profile rules out horizontal orientation of the triblock copolymer chain.

Although the depth profile leaves vertical orientation as the only alternative and it is not surprising that the top surface is enriched with PEG on account of its lower surface energy than that of PPE, the details of chain arrangement in the film are quite complex for the following reasons. The thickness of the film, ~70 nm in Figure 5a, far exceeds the fully extended length of the triblock copolymer chain of about 39 nm. Thus, a chain with a PEG block near either the top or the bottom surface cannot span the entire thickness of the film. Nor is it likely that a large fraction of such chains can be stacked vertically in tandem because such arrangement would call for a third intense oxygen density peak in the middle of the film which was not observed experimentally. On the basis of these considerations, a picture of chain arrangement is proposed in Figure 6 in which neighboring chains overlap in the vertical direction to result in top and bottom regions very rich in oxygen because they consist mainly of PEG and the middle region less rich in oxygen because it contains both PEG and PPE. The arrangement of chains so depicted predicts a depth profile in general agreement with experimental results.

When the triblock copolymer was blended with PMMA which also contained oxygen atoms, the oxygen counts were higher throughout the film, as can be seen in Figure 5b,c for the 50/50 and 20/80 blends. But the essential feature of two oxygen-rich regions near the top and bottom surfaces remained; i.e., the chain arrangement represented by Figure 6 is also applicable. Compared to the 50/50 blend, the 20/80 blend has a more intense oxygen density at the first peak (shallow depth). This indicates that more PEG segments are positioned near the air–film interface. The difference between the two blends is probably related to the dynamics of the phase separation process. When the triblock copolymer content was reduced to 10 or 2%, the oxygen count came mostly from PMMA, and no relevant information could be extracted.

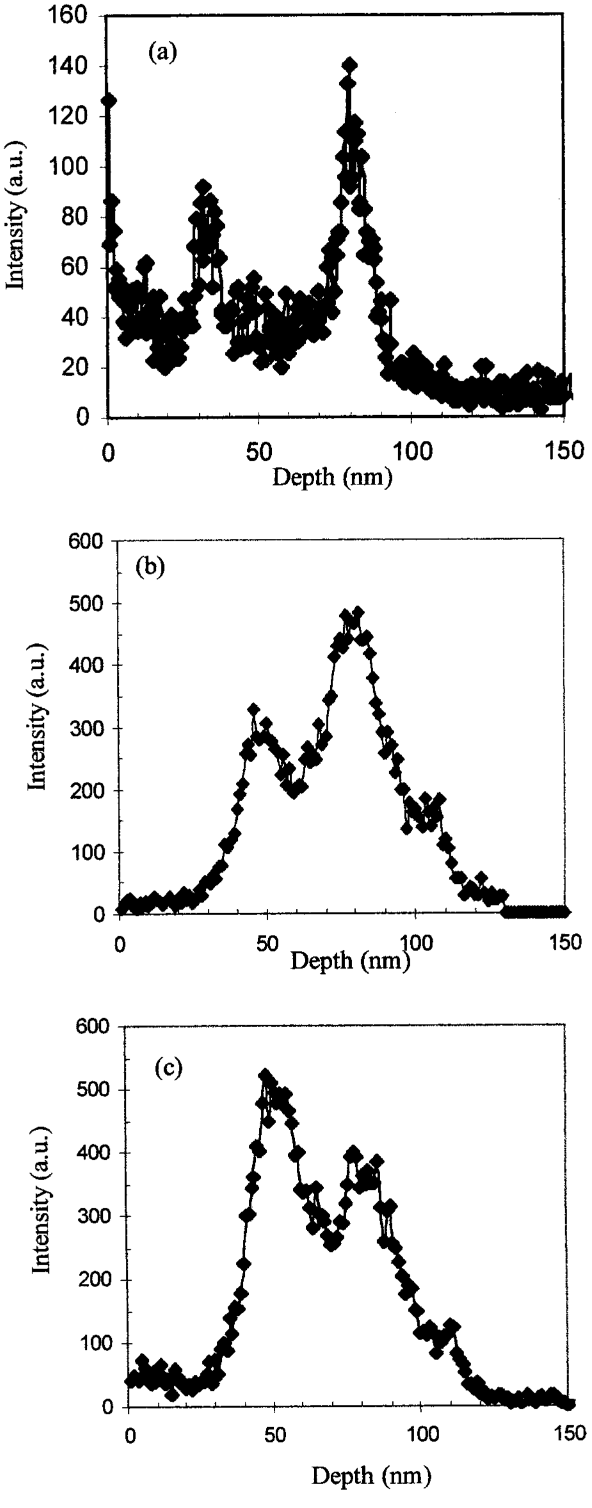

Figure 5. Depth profiles from oxygen SIMS measurements for (a) PPEPEG pristine film and PPEPEG/PMMA binary blend films: (b) 50/50 and (c) 20/80. The substrates were etched with HF to remove the native oxide layer.

D. Atomic Force Microscopy (AFM). Although the SIMS results on oxygen depth profile confirm vertical orientation of the triblock copolymer in the films, they provide no information on morphology or phase relationships. Atomic force microscopy which probes surface morphology complements the studies of molecular orientation by fluorescence polarization and SIMS. In parts a and b of Figure 7, AFM images of a 20/80 triblock/PMMA blend are shown in the morphology mode and contact mode, respectively. The morphology mode maps the height contour, the bright regions being nearer the top than the darker ones. The image in Figure 7a clearly shows two phases, with domain size on the order of 2 μm. However, the morphology image does not identify the compositions of the bright and dark areas. The answer comes from measurement in the contact mode. In the contact mode, the image maps the friction contour and therefore differentiates phase compositions. In Figure 7b, the bright regions can be identified as PMMA phase because they are much more abundant than the dark areas. In comparing parts a and b of Figure 7, it is seen that the bright and dark areas are reversed; i.e., the dark areas in Figure 7a represent PMMA domains and the bright areas, which are nearer to the surface, represent the PEG-rich regions. The assignment of bright and dark areas was verified by washing the surface of the film with acetic acid to remove PMMA. After washing, the PEG-rich regions (bright) outweigh the PMMA regions (dark) in Figure 7c, and only the PEG-rich regions remain in Figure 7d. The results appear to embody features somewhat different from those of thick films; all three components are phase-separated, which is different from the situation in the thick films. If the above interpretation of the phase separation mechanism is correct, then the importance of the surface energy contribution to molecular organization and orientation in thin films speaks for itself.

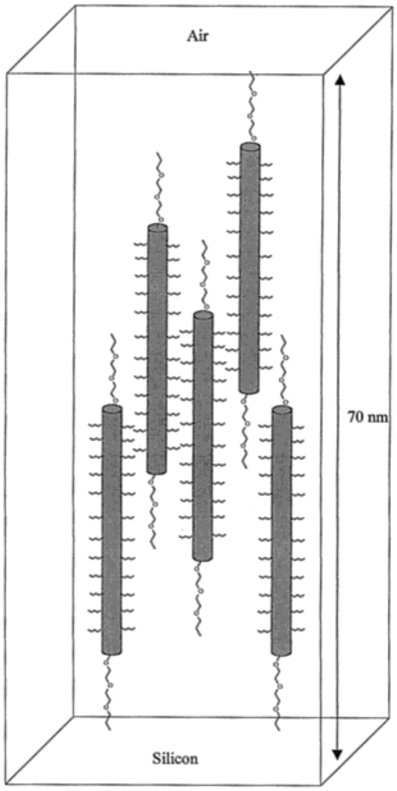

Figure 6. Proposed molecular organization for the PPEPEG thin film on silicon surface.

Conclusion

The combined results of fluorescence, secondary ion mass spectroscopy, and atomic force microscopy point to the following conclusions.

(1) In thin films of the triblock copolymer with a rigid π-conjugated polymer, poly(p-phenylene ethylene) and

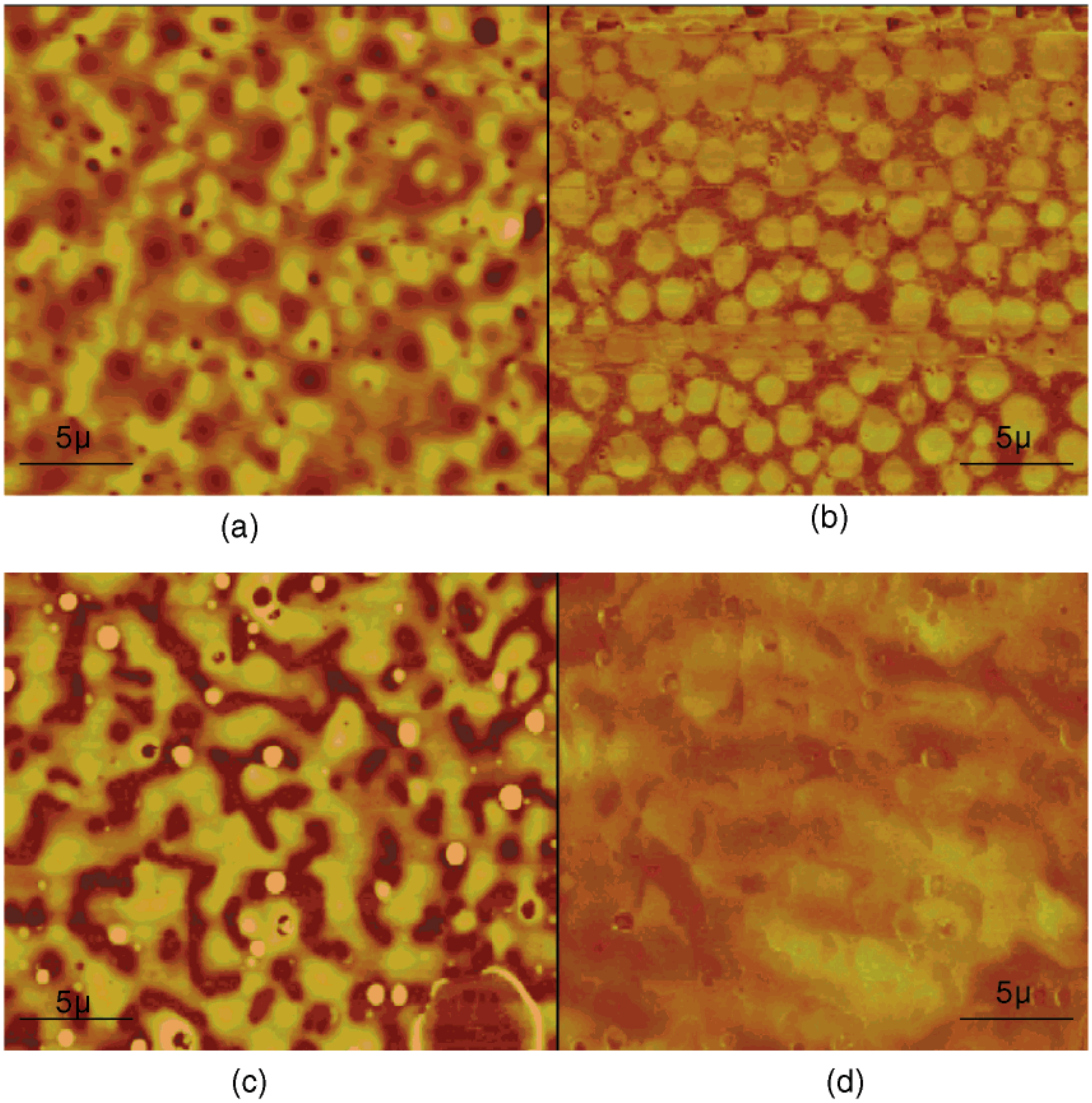

Figure 7. AFM images of 20/80 PPEPEG/PMMA binary blend films in both morphology and contact modes: (a) morphology mode, (b) contact mode, (c) after washing with acetic acid in morphology mode, and (d) after washing with acetic acid in contact mode.

poly(ethylene glycol) (PPEPEG) and its blends with PMMA, the copolymer molecules are oriented vertically to the silicon substrate surface.

(2) The rigid PPE middle blocks tend to aggregate even at the low concentration in PMMA blends. However, triblock copolymer chains are dispersed molecularly in the low concentration (~2 wt % copolymer in PMMA), leading to high fluorescence intensity at a wavelength typical of nonassociated molecules.

(3) The reinforced action of this rigid polymer for PMMA was obtained. The secant modulus of the 2 wt % blend in a tensile test was 5.7 times the value of PMMA.

(4) At the air−film interface of a 20/80 wt % PPEPEG−PMMA blend, regions of PEG groups are interspersed with regions of PMMA. The morphology of thin films can be pictured as bundles of vertically oriented triblock molecules, about 1−2 μm in size, distributed in the major phase of PMMA.

Acknowledgment. We thank the National Science Foundation, Division of Materials Research, under Grant DMR 9802108, for supporting this research.

References and Notes

(1) Fu, H.; Yun, H.; Kwei, T. K.; Okamoto, Y.; Blumstengel, S.; Walser, A.; Dorsinville, R. *Polym. Adv. Technol.* **1999**, *10*, 259.
(2) Huang, W. Y.; Yun, H.; Lin, H. S.; Kwei, T. K.; Okamoto, Y. *Macromolecules* **1999**, *32*, 8089.
(3) Huang, W. Y.; Gao, W.; Kwei, T. K.; Okamoto, Y. *Macromolecules* **2001**, *34*, 1570.
(4) Kloppenburg, L.; Jones, D.; Bunz, U. H. F. *Macromolecules* **1999**, *32*, 4194.
(5) Kloppenburg, L.; Jones, D.; Claridge, J. B.; zur Loye, H. C.; Bunz, U. H. F. *Macromolecules* **1999**, *32*, 4460.
(6) Bunz, U. H. F.; Enkelmann, V.; Kloppenburg, L.; Jones, D.; Shimizu, K. D.; Claridge, J. B.; Zur Loye, H.-C.; Lieser, G. *Chem. Mater.* **1999**, *11*, 1416.
(7) Bunz, U. H. F.; et al. *Chem. Rev.* **2000**, *100*, 1605.
(8) Halkyard, C. E.; Rampey, M. E.; Kloppenburg, L.; Studer-Martinez, S. L.; Bunz, U. H. F. *Macromolecules* **1998**, *31*, 8656.
(9) Li, Hong; Powell, D. R.; Hayashi, R. K.; West, R. *Macromolecules* **1998**, *31*, 52.
(10) Weder, C.; Wrighton, M. S. *Macromolecules* **1996**, *29*, 5175.
(11) Moroni, M.; Le Moigne, J.; Luzzati, S. *Macromolecules* **1994**, *27*, 562.
(12) Palmans, A. R. A.; Smith, P.; Weder, C. *Macromolecules* **1999**, *32*, 4677.
(13) Ziener, U.; Godt, A. *J. Org. Chem.* **1997**, *62*, 6137.
(14) Montali, A.; Smith, P.; Weder, C. *Synth. Met.* **1998**, *Sept 15*, 123.

(15) Weder, C.; Sarwa, C.; Montali, A.; Bastiaansen, C.; Smith, P. *Science* **1998**, *279*, 835.

(16) Brandrup, J.; Immergut, E. H. *Polymer Handbook* 1989, 3rd ed., VI/356.

(17) Liberman, S. A.; Gomes, A. de S.; Macchi, E. M. *J. Polym. Sci., Polym. Chem. Ed.* **1984**, *22*, 2809.

(18) Martuscellie, E.; Demma, G. B. *Polymer Blends: Processing, Morphology, and Properties*; Plenum: New York, 1980; p 101.

(19) Shih, H. Y.; Kuo, W. F.; Pearce, E. M.; Kwei, T. K. *Polym. Adv. Technol.* **1995**, *6*, 413.

(20) Leclére, Ph.; Marsitzky, D.; Francke, V.; Setayesh, S.; Müllen, K.; Brédas, J. L.; Lazzaroni, R. *Polym. Prepr.* **2000**, *41* (2), 1483.

(21) Jenekhe, S. A.; Chen, X. L. *Science* **1998**, *279*, 1903.

(22) Jenekhe, S. A.; Chen, X. L. *Science* **1999**, *283*, 372.

(23) Muthukumar, M.; Ober, C. K.; Thomas, E. L. *Science* **1997**, *277*, 1225.

(24) Raphael, E.; de Gennes, P. G. *Makromol. Chem. Macromol. Symp.* **1992**, *62*, 1.

(25) Williams, D. R. M.; Fredrickson, G. H. *Macromolecules* **1992**, *35*, 3561.

(26) Halperin, A. *Macromolecules* **1990**, *23*, 2724.

(27) Semenov, A. N. *Mol. Cryst. Liq. Cryst.* **1991**, *209*, 191.

(28) Schwarz, S. A.; Wilkens, B. J.; Pudensi, M. A. A.; Rafailovich, M. H.; Sokolov, J.; Zhao, X.; Zhao, W.; Zheng, X.; Russell, T. P.; Jones, R. A. L. *Mol. Phys.* **1992**, *76*, 937.

(29) Zhao, J. Q.; Pearce, E. M.; Kwei, T. K. *Macromolecules* **1997**, *30*, 7119.

(30) Lowenhaupt, B.; Steurer, A.; Hellmann, G. P.; Gallot, Y. *Macromolecules* **1994**, *27*, 908.

MA010375K